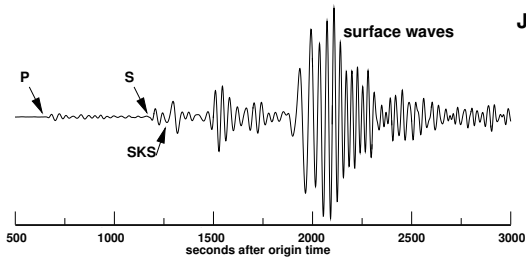


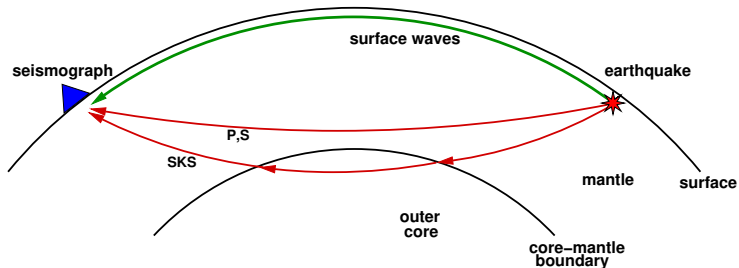
## Concepts developed in this lecture

- The free surface boundary conditions give rise to interference waves which propagate parallel to the surface and whose amplitude decays with depth.
- There are two classes of surface waves: Rayleigh waves which are constructively-interfering P- and SV-waves, and Love waves which are constructively-interfering SH-waves.
- Rayleigh waves exist in a uniform half-space; Love waves exist only for a structure where the wave speed of the material increases with depth.
- Surface waves in the Earth are dispersive and their propagation is described by the phase velocity and the group velocity.

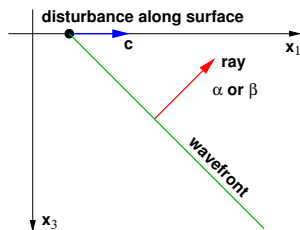
# Rayleigh waves



J.W. Strutt (L. Rayleigh)  
(1842–1919)



## Rayleigh waves in a homogeneous half-space



For the first case we look at P- and SV-waves interacting at the surface of a uniform half-space. The displacements in terms of the potentials are

$$u_1 = \phi_{,1} - \psi_{2,3} \quad u_2 = \psi_{1,3} - \psi_{3,1} \quad u_3 = \phi_{,3} + \psi_{2,1}$$

For a monochromatic wave of frequency  $\omega$  propagating in the  $x_1$  direction with velocity  $c$ , the potentials  $\phi$  and  $\psi$ , and the displacement  $u_2$  are

$$\phi = f(x_3)e^{i(\omega t - kx_1)} \quad \psi = g(x_3)e^{i(\omega t - kx_1)} \quad u_2 = h(x_3)e^{i(\omega t - kx_1)}$$

## Rayleigh waves in a homogeneous half-space

The amplitude dependence with depth is given by the terms  $f(x_3)$ ,  $g(x_3)$  and  $h(x_3)$  and  $k = \omega/c$  is the wavenumber.

Substituting these in the wave equations for  $\phi$ ,  $\psi$  and  $u_2$  gives

$$f'' + k^2 r_\alpha^2 f = 0 \quad g'' + k^2 r_\beta^2 g = 0 \quad h'' + k^2 r_\beta^2 h = 0$$

where

$$r_\alpha = \left[ \frac{c^2}{\alpha^2} - 1 \right]^{1/2} \quad r_\beta = \left[ \frac{c^2}{\beta^2} - 1 \right]^{1/2}$$

The solution for the first equation is

$$f(x_3) = A e^{-ikr_\alpha x_3} + A' e^{ikr_\alpha x_3} = A e^{-ikr_\alpha x_3}$$

with similar solutions for  $g$  and  $h$  but with  $r_\alpha$  replaced with  $r_\beta$ .

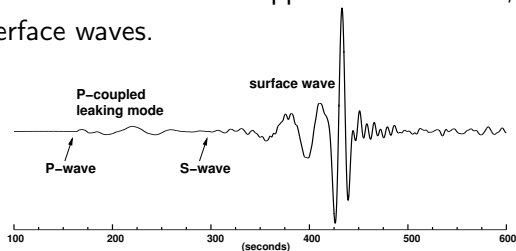
Surface waves have an amplitude which decreases with depth, so

$r_\alpha$  must be imaginary and  $A' = 0$ .

# Rayleigh waves in a homogeneous half-space

There are three cases:

- If  $\beta < \alpha < c$ , then both  $r_\alpha$  and  $r_\beta$  are real and both P- and S-waves reflect from the surface and propagate back into the half-space as body-waves.
- If  $\beta < c < \alpha$ , then  $r_\alpha$  is imaginary,  $r_\beta$  is real, then P-waves are trapped at the surface but S-waves reflect from the surface and propagate back into the half-space.
- If  $c < \beta < \alpha$ , then both  $r_\alpha$  and  $r_\beta$  are imaginary, then both P- and S-waves are trapped at the surface, giving rise to interface waves.



## Rayleigh waves in a homogeneous half-space

Substituting the amplitude terms  $f(x_3)$  etc., the potentials  $\phi$  and  $\psi$  and displacement  $u_2$  are

$$\phi = Ae^{[-ikr_\alpha x_3 + ik(x_1 - ct)]} \quad \psi = Be^{[-ikr_\beta x_3 + ik(x_1 - ct)]} \quad u_2 = Ce^{[-ikr_\beta x_3 + ik(x_1 - ct)]}$$

To evaluate  $A$ ,  $B$  and  $C$  we apply the free surface boundary condition  $\sigma_{13} = \sigma_{23} = \sigma_{33} = 0$ . Substituting the potentials for the displacements in the free surface boundary condition at  $x_3 = 0$

$$2\phi_{,31} + \psi_{,11} - \psi_{,33} = 0 \quad (\lambda + 2\mu)\phi_{,33} + \lambda\phi_{,11} + 2\mu\psi_{,13} = 0 \quad u_{2,3} = 0$$

Substituting  $u_2$  in the equation for  $u_{2,3}$  gives  $C = 0$ . Therefore, the surface wave in a half-space has no transverse (SH) component of motion.

## Rayleigh waves in a homogeneous half-space

Substituting the potentials in the remaining boundary conditions

$$2r_\alpha A - (1 - r_\beta^2)B = 0$$

$$\alpha^2(r_\alpha^2 + 1) - 2\beta^2]A - 2\beta^2 r_\beta B = 0$$

This  $2 \times 2$  system of homogeneous linear equations has a non-trivial solution when its determinate is zero, giving

$$[\alpha^2(r_\alpha^2 + 1) - 2\beta^2] (1 - r_\beta^2) - 4r_\alpha r_\beta \beta^2 = 0$$

and substituting for the values of  $r_\alpha$  and  $r_\beta$  gives

$$\left[2 - \frac{c^2}{\beta^2}\right]^2 = 4 \left[1 - \frac{c^2}{\beta^2}\right]^{1/2} \left[1 - \frac{c^2}{\alpha^2}\right]^{1/2}$$

## Rayleigh waves in a homogeneous half-space

For the case of a Poisson solid ( $\lambda = \mu$ , and  $\alpha^2/\beta^2 = 3$ )

$$\frac{c^2}{\beta^2} \left[ \frac{c^6}{\beta^6} - 8 \frac{c^4}{\beta^4} + \frac{56c^2}{3\beta^2} - \frac{32}{3} \right] = 0$$

This equation has four real roots:

- $c^2/\beta^2 = 0$  – no physical significance,
- $c^2/\beta^2 = 4$  –  $\beta < \alpha < c$  – reflected wave,
- $c^2/\beta^2 = 2 + 2/\sqrt{3}$  –  $\beta < \alpha < c$  – reflected waves,
- $c^2/\beta^2 = 2 - 2/\sqrt{3} = 0.8453$  – evanescent wave.

For this case

$$c = 0.9194\beta$$

The apparent velocity of the Rayleigh wave in a homogeneous Poisson solid half-space is independent of frequency and is  $\sim 0.92$  the shear wave speed of the medium.



## Rayleigh waves in a homogeneous half-space

For a Poisson solid  $r_\alpha = 0.85i$  and  $r_\beta = 0.39i$  and substituting in the expressions for the wave amplitude and taking the real part of the displacement gives

$$u_1 = -Ak \sin(\omega t - kx_1)(e^{0.85kx_3} - 0.58e^{0.39kx_3})$$

$$u_3 = -Ak \cos(\omega t - kx_1)(-0.85e^{0.85kx_3} + 1.47e^{0.39kx_3})$$

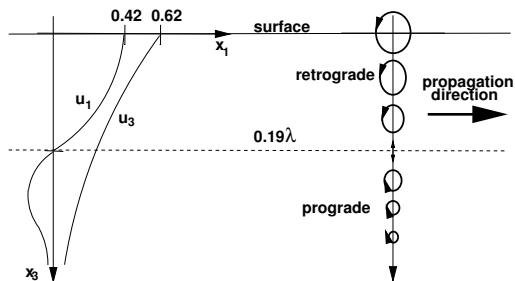
At the surface  $x_3 = 0$  and these become

$$u_1 = 0.42a \sin(\omega t - kx_1)$$

$$u_3 = 0.62a \cos(\omega t - kx_1)$$

where  $a = -Ak$ . Then the Rayleigh wave is polarized in the vertical-radial plane; the horizontal component leads the vertical component of motion by  $\pi/2$  and the amplitude of the vertical component is about 1.5 times the amplitude of the horizontal component. Therefore, the Rayleigh wave has retrograde elliptical particle motion.

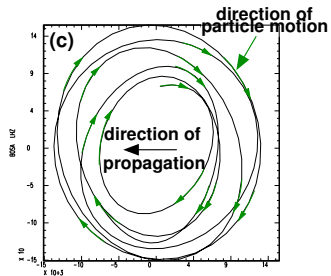
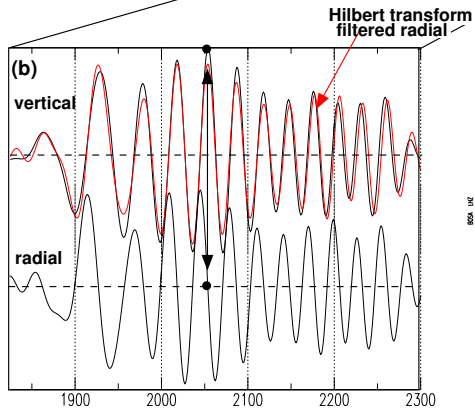
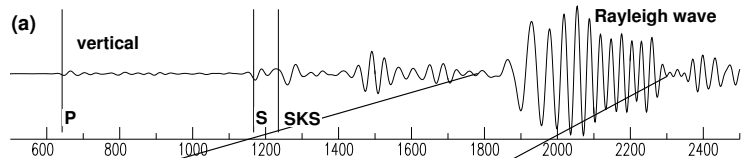
## Rayleigh waves in a homogeneous half-space



The particle displacement is the same for all frequencies, but the absolute values depend on  $\omega$  or  $\lambda$ .

Since the decay of displacement with depth is controlled by factors like  $\exp(-k_1 x_3) = \exp(-2\pi x_3 / \lambda)$ , long wavelength Rayleigh waves penetrate deeper than shorter wavelength Rayleigh waves.

# Observed Rayleigh waves



# Lamb's problem

**Lamb (1904)** extended Rayleigh's results by finding the complete response of a homogeneous half-space to a vertical point force acting on the surface of the half-space.

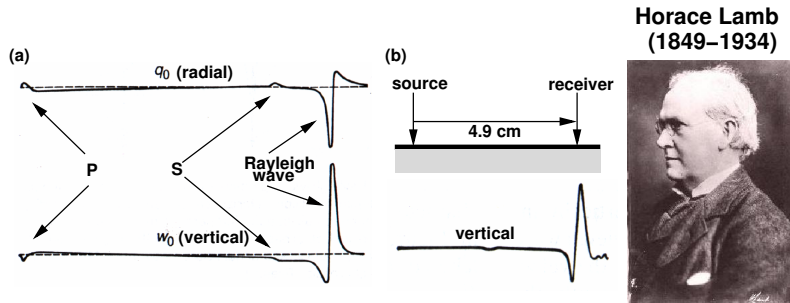
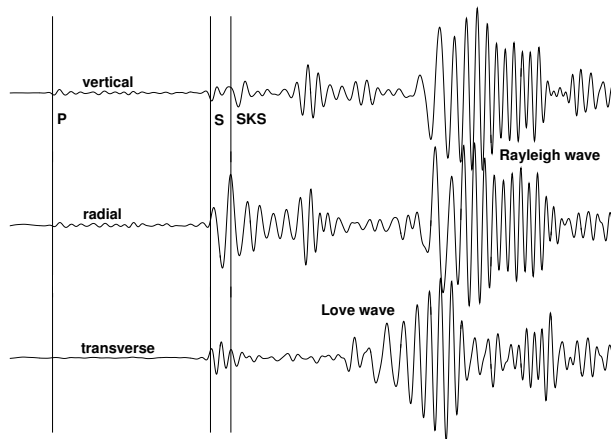


**Figure:** Lamb's Problem. (a) Lamb's transient solution to an impulsive vertical point force applied to the surface of a half-space; (b) recording of the vertical motion from a vertical point force on the surface of a half-space. (adapted from Ewing *et al*, 1957)

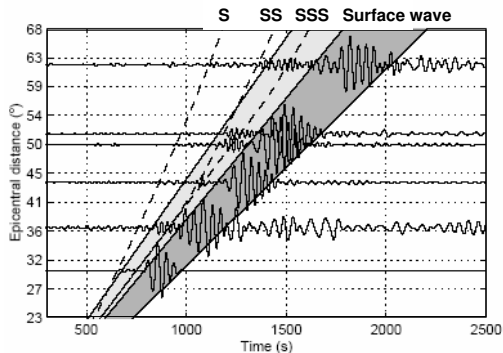
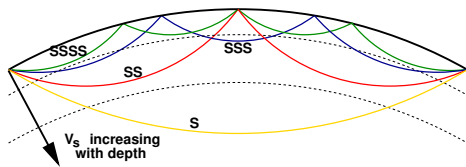
# Love waves



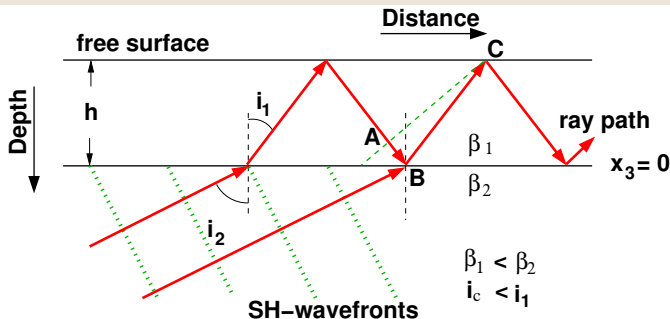
**A.E.H. Love**  
(1863–1940)



# Love waves – Multiple surface reflecting S-waves



## Love wave period equation



There is no phase shift in the wavefront when it reflects from the free surface. The phase shift on reflecting from the interface at B is  $\Theta = 2 \tan^{-1}(\mu_2 r_{\beta_2}^* / \mu_1 r_{\beta_1})$ . The phase delay along the path ABC is  $-k_{\beta_1}$  times the path length

$$\begin{aligned}
 -k_{\beta_1}(BC \cos 2i_1 + h / \cos i_1) &= -k_{\beta_1}(h \cos 2i_1 / \cos i_1 + h / \cos i_1) \\
 &= -2hk_{\beta_1} \cos i_1
 \end{aligned}$$

## Love wave period equation

For constructive interference to occur

$$2 \tan^{-1} \left( \frac{\mu_2 r_{\beta_2}^*}{\mu_1 r_{\beta_1}} \right) - 2hk_{\beta_1} \cos i_1 = 2n\pi$$

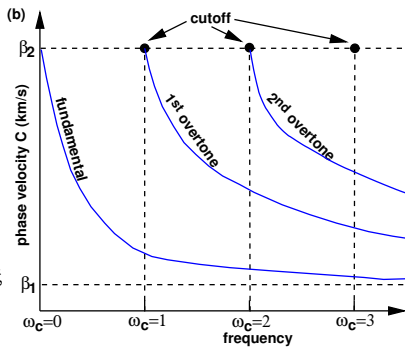
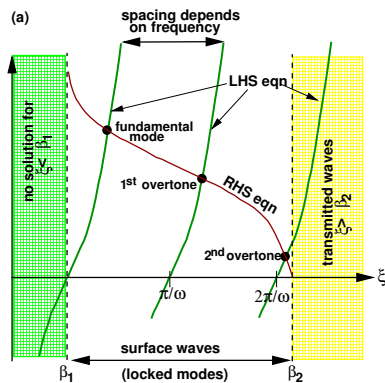
or

$$\tan(hk_{\beta_1} \cos i_1) = \tan(hk_{\beta_1} r_{\beta_1}) = \frac{\mu_2 r_{\beta_2}^*}{\mu_1 r_{\beta_1}}$$

which is the Love wave period equation. For this case the waves are dispersive,  $c(\omega)$ . The tangent has positive values between zero and  $\infty$  for various intervals of  $kr_{\beta_1}h$ , the first for  $0 \rightarrow \pi/2$  which corresponds to the fundamental mode, the second for  $\pi \rightarrow 3\pi/2$  which corresponds to the first higher mode, and so on. **Both the dispersion and the modes come from the finite dimension of the layer.**



# Love wave period equation



## Love wave period equation

The period equation has real roots only for  $\beta_1 < c < \beta_2$ .

The right side is independent of  $\omega$ ; the left side is periodic and has zeros at  $\xi = n\pi/\omega$ . The  $n = 1$  tangent curve enters the range when  $\pi/\omega_{c1} = (h/\beta_1)(1 - \beta_1^2/\beta_2^2)^{1/2}$ . For  $\omega$  higher than  $\omega_{c1}$ , two Love waves exist, both having the same frequency but with different velocities.

The  $n^{\text{th}}$  curve enters from the right when

$$\omega = \frac{n\pi\beta_1}{h} \left(1 - \frac{\beta_1^2}{\beta_2^2}\right)^{-1/2} = \omega_{cn}$$

## Love wave particle motion with depth

The displacements for the Love wave are

$$u_2^L = (B_1 e^{ikr_{\beta_1} x_3} + B_1' e^{-ikr_{\beta_1} x_3}) e^{ik(x_1 - ct)}$$

$$u_2^{HS} = B_2 e^{-ikr_{\beta_2} x_3} e^{ik(x_1 - ct)}$$

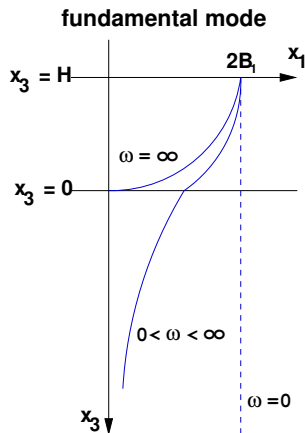
Using the boundary conditions at the surface and interface, the displacements are

$$u_2^L = 2B_1 \cos \left[ kr_{\beta_1} h \left( 1 - \frac{x_3}{h} \right) \right] \cos[k(r_{\beta_1} h + x_1 - ct)]$$

$$u_2^{HS} = 2B_1 \cos(kr_{\beta_1} h) e^{ikr_{\beta_2}^* x_3} \cos[k(r_{\beta_1} h + x_1 - ct)]$$

where  $r_{\beta_2}^* = i(1 - c^2/\beta^2)^{1/2}$ . In the half-space the displacement decreases exponentially with depth; in the layer the displacement varies with depth depending on  $kr_{\beta_1} h$  with a different variation for each mode.

## Love wave particle motion with depth



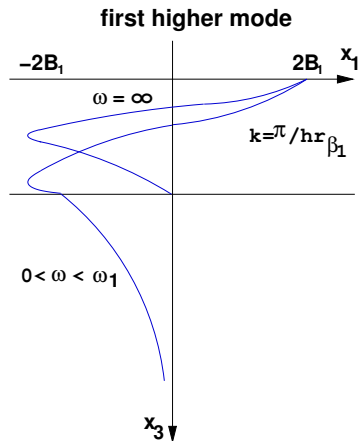
For the fundamental mode

$$k = 0 \quad |u_2| = 2B_1 \quad \text{for all values of } x_3$$

$$k = \infty \quad |u_2| = \begin{cases} 2B_1 & \text{for } x_3 = h \\ 0 & \text{for } x_3 = 0 \end{cases}$$

At  $x_3 = h$ ,  $u_2 = 2B_1$  for all  $\omega$ , at  $x_3 = 0$ ,  $0 \leq u_2 \leq 2B_1$  for  $\infty \geq \omega \geq 0$ , and in the half-space  $u_2$  decays exponentially with depth.

# Love wave particle motion with depth



For the first higher mode

$$\pi \leq kr_{\beta_1} h \leq 3\pi/2$$

$$k = \pi / r_{\beta_1} h \quad |u_2| = \begin{cases} 2B_1 & \text{for } x_3 = h \\ 0 & \text{for } x_3 = h/2 \\ -2B_1 & \text{for } x_3 = 0 \end{cases}$$

$$k = \infty \quad |u_2| = \begin{cases} 2B_1 & \text{for } x_3 = h \\ 0 & \text{for } x_3 = 2h/3 \\ -2B_1 & \text{for } x_3 = h/3 \\ 0 & \text{for } x_3 = 0 \end{cases}$$

## Group velocity

The displacement of a dispersive wave with a continuous distribution of frequencies is given by

$$u(x, t) = \int_{-\infty}^{\infty} A(k) e^{i(kx - \omega t)} dk$$

The amplitude  $A(k)$  of the integrand varies slowly compared to the phase  $(kx - \omega t)$  and there is only a contribution to the amplitude of the wave for values of  $x$  and  $t$  when the phase is stationary. In this case

$$\frac{d\Phi}{dk} = \frac{d}{dk}(kx - \omega t) = x - \frac{d\omega}{dk}t = x - Ut = 0 \quad \longrightarrow \quad U = \frac{x}{t}$$

This is the group velocity corresponding to the frequency  $\omega_0$  or wavenumber  $k_0$  which makes the phase stationary. At this point and time there is a contribution to the seismogram  $u(x, t)$ .

## Group velocity

To determine the amplitude we expand the argument in a Taylor series about  $\omega_0$

$$kx - \omega t = (k_0x - \omega_0t) + (k - k_0) \frac{d}{dk} [kx - \omega t]_{k=k_0} \\ + \frac{1}{2} (k - k_0)^2 \frac{d^2}{dk^2} [kx - \omega t]_{k=k_0} + \dots$$

For a point where the phase is stationary, the first derivative is zero and using  $\frac{d}{dk} (kx - \omega t) = x - Ut$ , the integral becomes

$$u(x, t) = A(k_0) e^{i(k_0x - \omega_0t)} \int_{-\infty}^{\infty} \exp \left\{ i \frac{1}{2} (k - k_0)^2 \frac{dU}{dk} t \right\} dk$$

Making the change of variable  $\xi^2 = (1/2)(k - k_0)^2 (dU/dk)t$

$$u(x, t) = A(k_0) e^{i(k_0x - \omega_0t)} \left[ \frac{t}{2} \frac{dU}{dk} \right]_{k_0}^{-1/2} \int_{-\infty}^{\infty} e^{-i\xi^2} d\xi \\ = A(k_0) e^{i(k_0x - \omega_0t)} \left[ \frac{t}{2} \frac{dU}{dk} \right]_{k_0}^{-1/2} (i\pi)^{1/2}$$

## Group velocity

Taking the real part we obtain

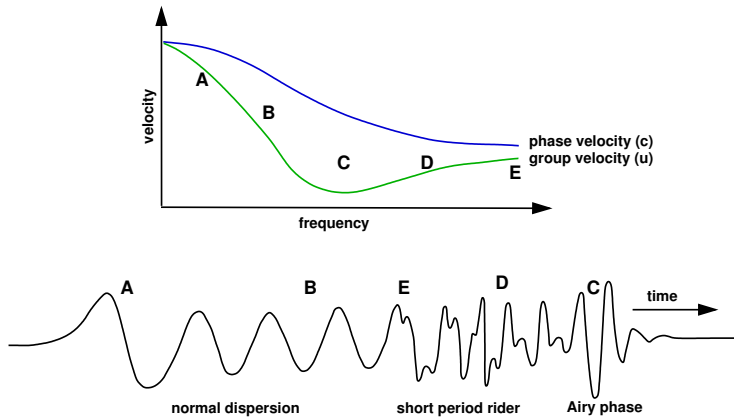
$$u(x, t) = A(k_0) \left[ \frac{2\pi}{(x/U) (dU/dk)} \right]^{1/2} \cos(k_0 x - \omega_0 t \pm \pi/4)$$

Then for a given  $x$  and  $t$ , energy is contained in a cosine wave of frequency  $k_0$  or  $\omega_0$  corresponding to  $d\Phi/d\omega = 0$ . The largest amplitude corresponds to  $dU/dk = 0$  and is called the Airy phase. When the second derivative is zero, we need the next term in the Taylor expansion. The Airy phase amplitude is

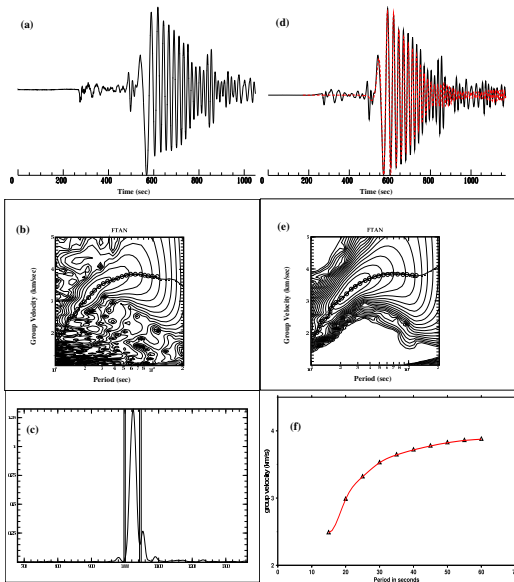
$$u(x, t) = A(k_0) \left[ \frac{2\pi}{(x/U) (d^2U/dk^2)} \right]^{1/3} \cos(k_0 x - \omega_0 t \pm \pi/4)$$



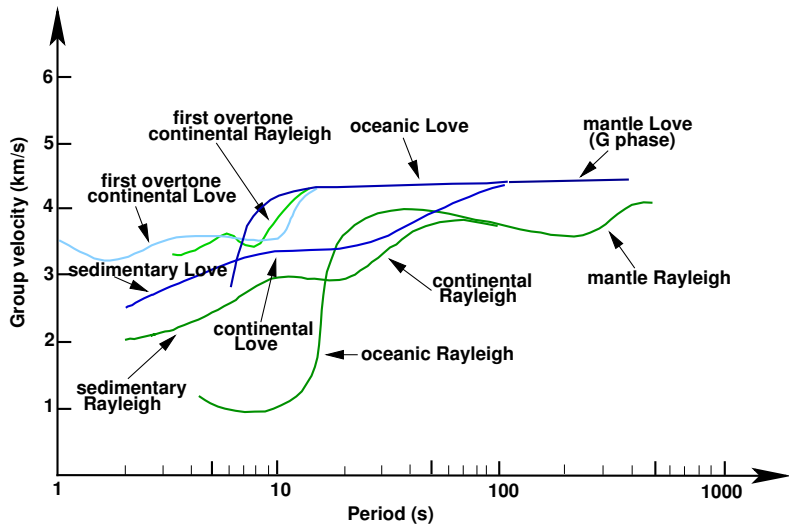
# Group velocity



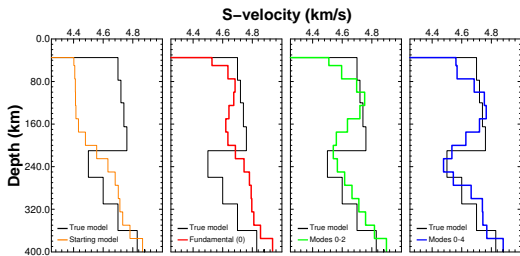
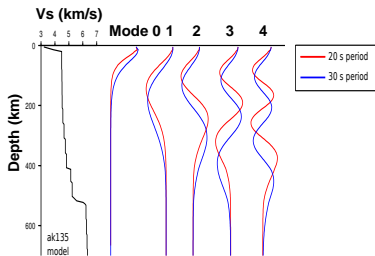
# Observed group velocity



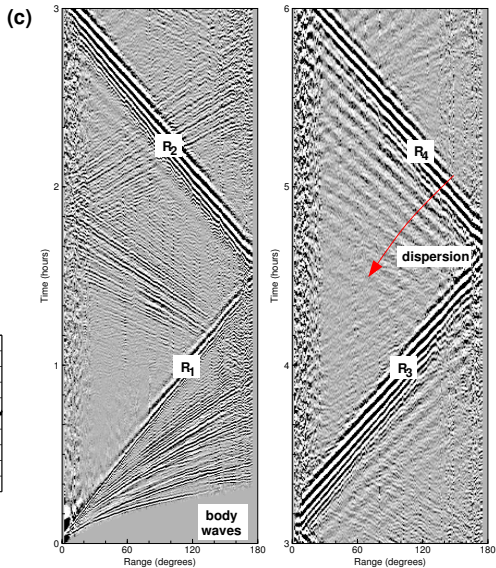
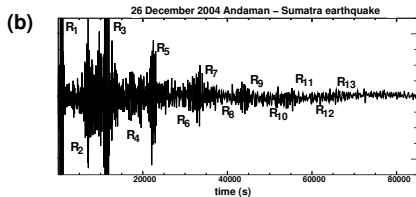
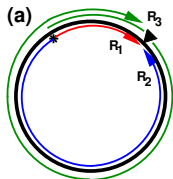
# Observed group velocity



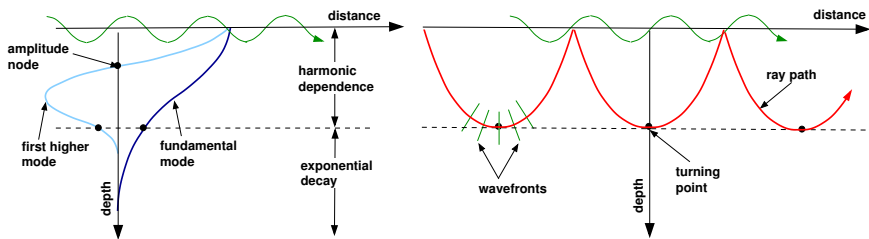
# Depth resolution



# Spherical Earth model



# Correspondence between rays and modes

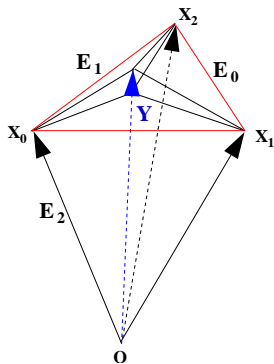
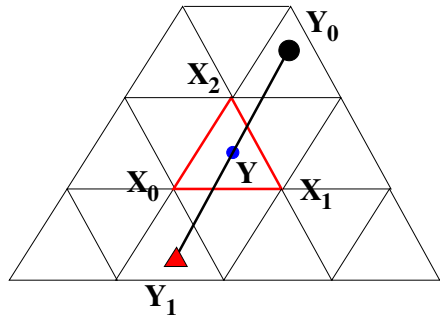


## Surface wave summary

- The free surface boundary conditions give rise to interference waves which propagate parallel to the surface and whose amplitude decays with depth.
- There are two classes of surface waves: Rayleigh waves which are constructively-interfering P- and SV-waves and Love waves which are constructively-interfering SH-waves.
- Rayleigh waves exist in a uniform half-space; Love waves exist only for a structure where the wave speed of the material increases with depth.
- Surface waves in the Earth are dispersive and their propagation is described by the phase velocity and the group velocity.

## Surface wave tomography

The region of interest is gridded by a two-dimensional finite element mesh of triangular elements with sides of length  $1^\circ$  on a spherical surface. Each node point of the triangular element is defined by a position vector from the center of the Earth.





## Surface wave tomography

The velocity/slowness is calculated at the nodes of these triangles from intersecting earthquake-receiver paths for which Rayleigh wave group velocity dispersion measurements were made.

$$t = \int_{path} s \, dx \quad (1)$$

where the integral is over the source-receiver path and  $s$  is the slowness (inverse velocity). Summing over all triangles along the ray path

$$t = \sum_{i=1}^n \int_0^{l_i} s \, dx \quad (2)$$

where  $l_i$  denotes the length of the ray path segment within the  $i$ th triangle.

## Surface wave tomography

Within each triangle slowness at any given point  $\mathbf{X}$  along the ray path is given by:

$$s = \varepsilon_0 \cdot s_0(\mathbf{X}_0) + \varepsilon_1 \cdot s_1(\mathbf{X}_1) + \varepsilon_2 \cdot s_2(\mathbf{X}_2) \quad (3)$$

where  $\mathbf{X}_0$ ,  $\mathbf{X}_1$  and  $\mathbf{X}_2$  are the position vectors of node points of the triangle (labeled anti-clockwise) with the center of the Earth taken as the origin.

Substituting equation 3 in equation 2

$$t = \sum_{i=1}^n \left[ s_0(\mathbf{X}_0) \int_0^{l_i} \varepsilon_0 dx + s_1(\mathbf{X}_1) \int_0^{l_i} \varepsilon_1 dx + s_2(\mathbf{X}_2) \int_0^{l_i} \varepsilon_2 dx \right] \quad (4)$$

where  $\varepsilon_0$ ,  $\varepsilon_1$ ,  $\varepsilon_2$  are the weights assigned to the three nodes and  $\varepsilon_0 + \varepsilon_1 + \varepsilon_2 = 1$

# Surface wave tomography

Summing over the node points of the triangles, equation 4 can be re-written as:

$$t = \sum_{\text{points}} s(X) \sum_{\text{triangles}} \int \varepsilon dx \quad (5)$$

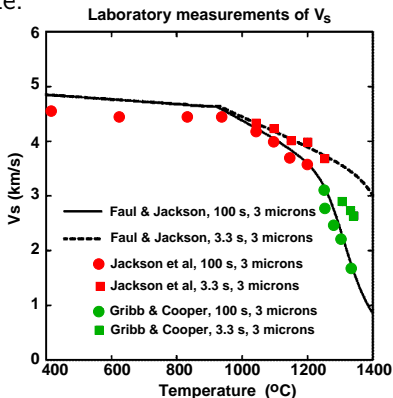
The forward problem can be expressed as:

$$\mathbf{d} = [\mathbf{A}] \mathbf{x} \mathbf{m} \quad (6)$$

where  $\mathbf{d}$  is an N-dimensional vector of travel time data ( $t$ ),  $\mathbf{m}$  is an M-dimensional vector that describes the model (slowness values at nodes) and  $[\mathbf{A}]$  is the operator that maps vectors in the model space into vectors in the data space.  $[\mathbf{A}]$  represents the numerical computation of distances for the formulation of the operator  $[\mathbf{A}]$ ). We invert the matrix  $[\mathbf{A}]$  to obtain the model vector  $\mathbf{m}$ .

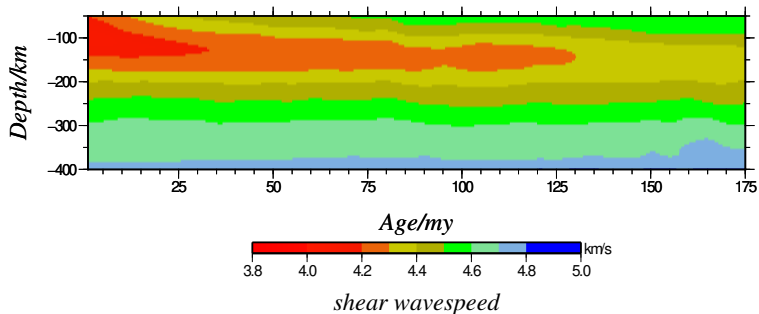
## $V_s$ vs $T$ relationship

Laboratory measurements of  $\mu$  for polycrystalline olivine at seismic frequencies show a strong decrease for temperatures considerably below the macroscopic solidus. They also show a strong dependence on grain size which is several orders of magnitude smaller in the laboratory experiments than the mantle grain size.



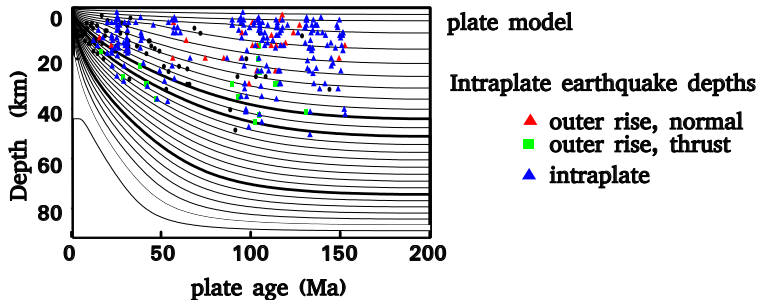
## $V_s$ vs $T$ relationship

Shear wave velocity beneath the Pacific Ocean, obtained from surface wave tomography using the fundamental and first five higher modes, averaged as a function of age.



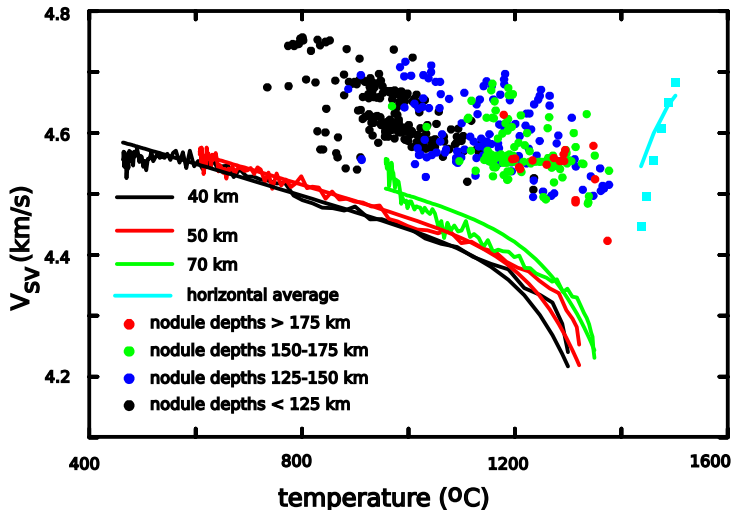
## $V_s$ vs $T$ relationship

Plate model for the oceanic lithosphere.



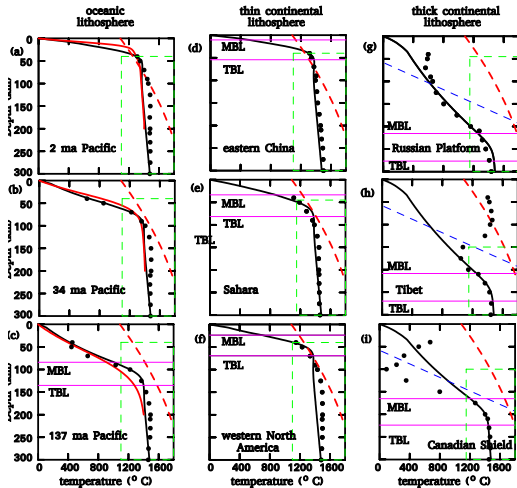
## $V_s$ vs $T$ relationship

Comparisons of the geophysical and petrological values of  $V_{sv}(T, z)$  used as constraints.



# Thermal lithosphere

Geotherms calculated from  $V_s v$  using the parameters from the fitting.

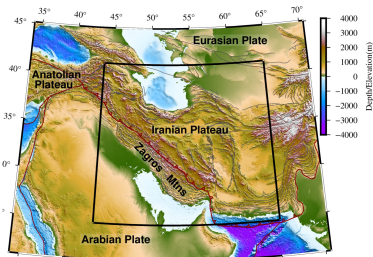
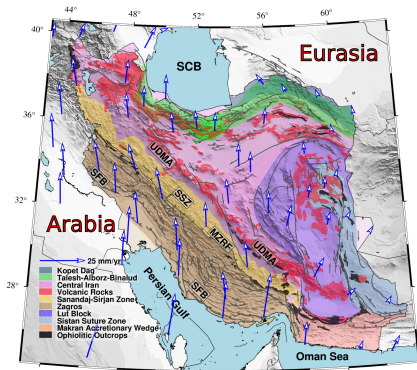




## Summary

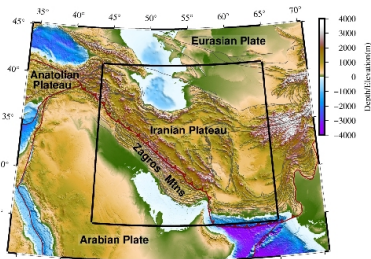
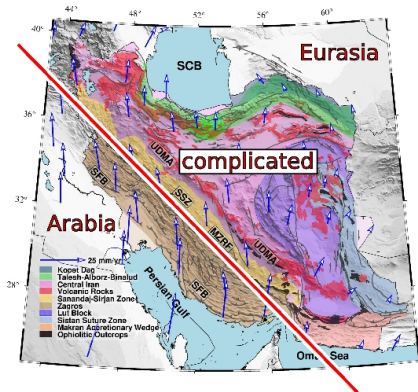
- Laboratory measurements of the  $\mu$  for polycrystalline olivine at seismic frequencies show a strong decrease in  $\mu$  with increasing  $T$  below the macroscopic solidus.
- This effect is probably due to stress relaxation on grain boundaries caused by diffusion.
- Laboratory experiments also show a strong dependence on grain size which is usually several orders of magnitude smaller in the laboratory experiments than in the mantle.
- This strong grain size-dependence makes it difficult to directly apply the laboratory results to mantle structure.
- Priestley & McKenzie took a simple empirical approach to relate seismic wave speed and temperature, allowing them to use the surface wave tomography results to map the upper mantle geotherm.

# An application of surface wave tomography



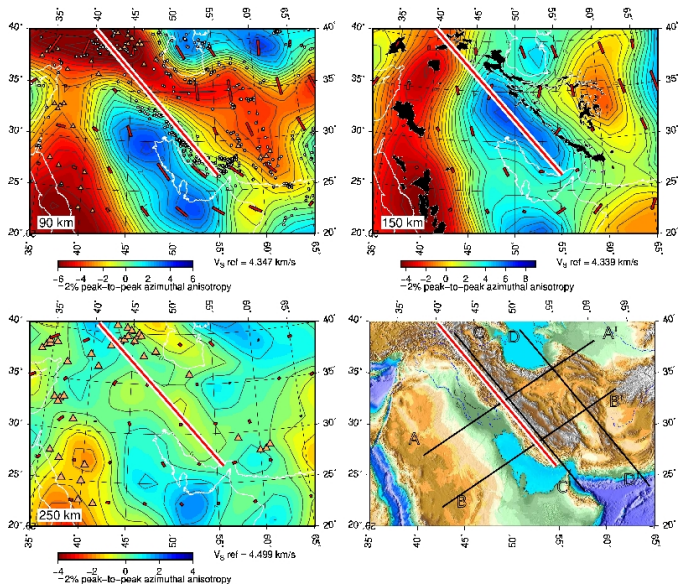
- SCB – South Caspian Basin
- UDMA – Urumieh-Dokhtar magmatic assemblage
- MZRF – Main Zagros Reverse Fault
- SSZ – Sanandaj-Sirjan Zone
- SFB – Simply Folded Belt

# An application of surface wave tomography

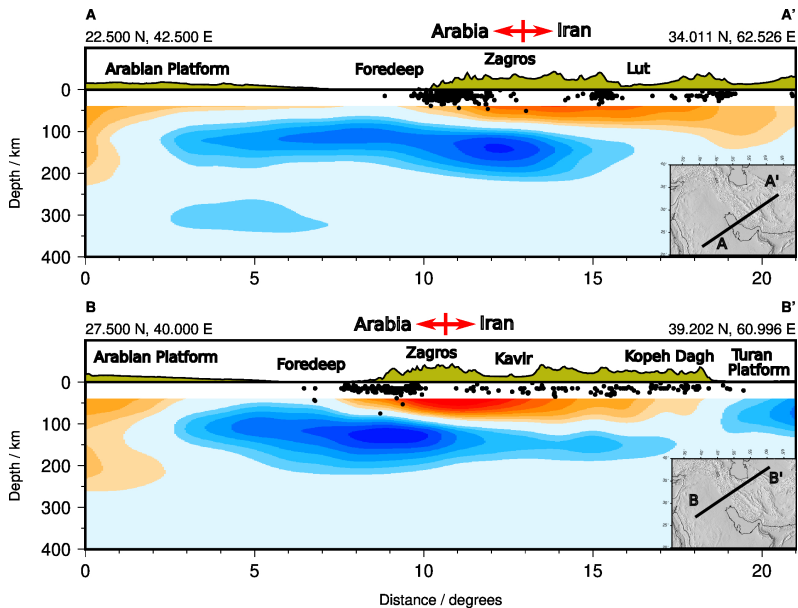


- SCB -- South Casplan Basin
- UDMA -- Urumieh-Dokhtar magmatic assemblage
- MZRF -- Main Zagros Reverse Fault
- SSZ -- Sanandaj-Sirjan Zone
- SFB -- Simply Folded Belt

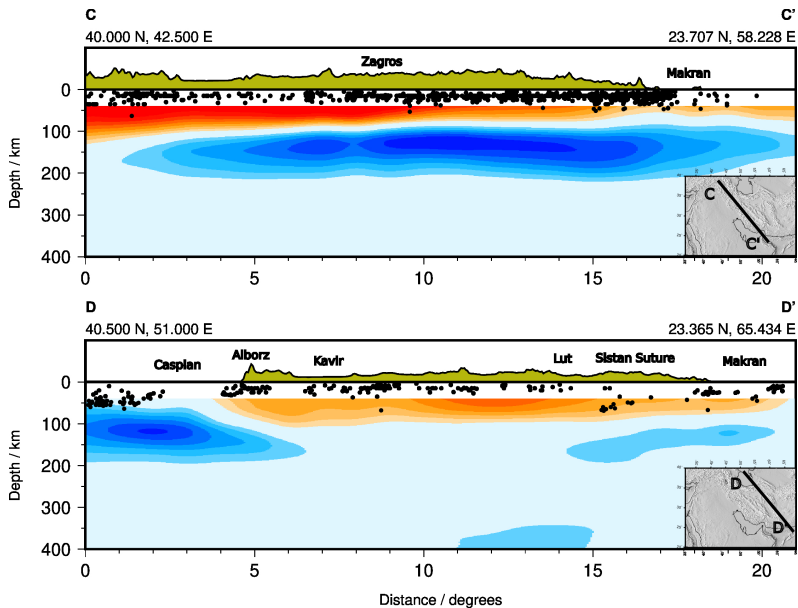
# An application of surface wave tomography



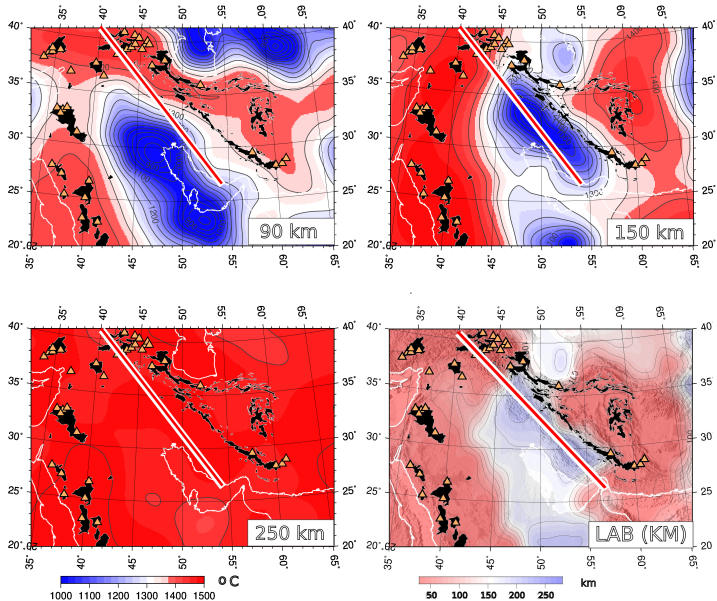
# An application of surface wave tomography



# An application of surface wave tomography



# An application of surface wave tomography



# An application of surface wave tomography

